Optimal design of cubic nonlinear energy harvester device for random vibrations

Optimal design of cubic nonlinear energy harvester device for random vibrations

V. De Biagi, B.M. Chiaia, G.C. Marano

Dept. of Structural, Geotechnical and Building Engineering, Politecnico di Torino, Corso Duca degli Abruzzi 24, 10129 Torino, Italy

Abstract

Linear energy harvesters have a narrow frequency bandwidth and hence operate efficiently only when the excitation frequency is very close to the fundamental frequency of the harvester. Consequently, small variations of the excitation frequency around the harvester's fundamental frequency drop the energy output making the harvesting process inefficient. To extend the harvester's bandwidth, some recent solutions call for using electromechanical devices with stiffness-type nonlinearities. This work deals with the optimisation of the performance of a single degree-of-freedom electromagnetic energy harvester whose mechanical behaviour has a Duffing-type nonlinearity, as for suspended masses, to reduce the size of energy harvesting devices without affecting their power output. The vibration input is assumed as a broadband Gaussian white noise base acceleration. It is analytically shown that the optimum load resistance of the device is different to that which is dictated by the principle of impedance matching.

Keywords: Energy Harvesting, Duffing-type nonlinearity, Ambient vibration, Threshold displacement, Optimization

1. Introduction

In recent years, much attention has been focused on the development of microelectromechanical systems (MEMS) which do not have to rely on external energy sources [1, 2]. The advantages of small self-powered sensors are numerous, especially when one considers large systems of sensors such as those that

are often used in structural health monitoring applications. In such cases, alleviating the need for an external energy source would eliminate the need for batteries which are often bulky and have a finite shelf-life [3]. Additionally, it may allow sensors to be placed in more hostile or inaccessible environments (such as inside rotating machinery or on bridges). To this end, the concept of harvesting electrical energy from mechanical vibrations has become a popular area of research [4]. With this aim in mind, a range of different energy harvesting devices has been developed for both MEMS scale and larger-scale systems. A review of such devices can be found in [5, 6]. In the first studies, an energy harvesting device relying on the electromagnetic induction that can be observed in a coil of wire when placed in a time varying magnetic flux (Faraday's law) was proposed [7]. To achieve this, a permanent magnet is attached to a vibrating base such that, when excited, the magnet oscillates within the coil. The device is modelled as a base excited mass-spring-damper where the damper is used to represent a combination of parasitic losses and the transfer of energy from the mechanical to the electrical domains. Subsequently, the dynamic response and the power output of other linear single-degree-of-freedom (SDOF) system devices to harmonic base excitations were analysed in several works. In [8] it is concluded that such an energy harvesting device would produce the most power if the damping caused by the electromagnetic coupling is equal to the mechanical damping present in the system, although that such a large coupling may be difficult to obtain. A detailed analysis of the ability of such devices to deliver power across a load resistor is also provided in [9]. It is concluded that maximum power output could be achieved when the coil resistance is equal to the damping due to the combination of mechanical and electrical losses in the device. While many of the afore mentioned works focus on the response of energy harvesting devices to sinusoidal excitations, it was soon realised that many ambient vibrations sources can actually be somewhat stochastic in nature. This led to a significant body of work which focused on the analysis of the response of energy harvesters to random excitations [10, 11, 12, 13, 14, 15, 16], something which is also be the focus of this paper.

With regards to the parasitic damping present in such a device it is intuitive to suggest that the minimisation of mechanical losses would maximise the energy available for transfer into the electrical domain. However, in Stephen [9] it is pointed out that a reduction in mechanical damping would lead to higher amplitude oscillations which may not be possible in small devices. As a result, Stephen concluded that the size is one of the main limiting factors with respect to energy harvester design - especially when considering devices which are designed to work alongside microelectromechanical systems.

Another conclusion that can be drawn from the literature is that several devices tailored to power maximisation only efficiently work if excited close to their resonance frequency and, therefore, they only perform well over a narrow bandwidth. As the dominant frequencies of most ambient vibrations are broadband, or time dependent, one can hypotheses that such a device will need to operate well over a larger bandwidth if it is to be used in many real world applications (the characteristics of several different types of ambient vibration are described in [17]).

Consequently, much effort has been directed towards the development of devices which are designed to work well over a larger bandwidth (reviews of which can be found in [18] and [19]). Of particular interest here are the findings shown in [20] where it is suggested that the introduction of Duffing-type nonlinearities into an SDOF electromagnetic device may help to extend its useful bandwidth. To achieve this, the centre magnet of the device is held in suspension by two outer magnets which were orientated such that their poles are repelling that of the centre magnet. It is shown that this configuration introduces a cubic spring term, similar to that of the mono-stable hardening spring Duffing oscillator. This nonlinearity has the effect of "skewing" the frequency response of the device which, it was hypothesised, may allow the device to function well over a larger bandwidth. Subsequently, in [21] the response of the device to a broadband white noise excitation is analysed using the Fokker-Planck-Kolmogorov (FPK) equation. It is concluded that the nonlinear stiffness term has no effects on the velocity probability density function of the centre magnet and, as

a result, has no benefit with regards to power output [22].

Although it is shown that Duffing-type nonlinearity can help in targeting the size of the energy harvesting device without affecting the power output [23, 24], limited studies on the optimal design of such a device when subjected to white noise excitation have been produced. A device able to harvest ambient vibrations, hence a broadband source, with controlled displacements, thus limited possibility for failure, would be expected [16]. Truong and colleagues proposed a system that limits the maximum displacement by modifying the electrical damping of the system [25]. For this purpose, the present paper deals with the response of a mono-stable device with Duffing-type nonlinearities considering a Gaussian white noise excitation. The main scope is the simultaneous optimisation of the electric power output and the mechanical maximum displacement (both of them in a stochastic measure). The electromechanical system was simplified by considering the effects of inductance negligible. The electromechanical system was thus modelled as a nonlinear SDOF system. A cubic nonlinearity with respect to the displacements was assumed - Duffing-like system - as it is a common case for vibrating cantilevers under large vertical displacements or similar mechanical systems. The input was assumed as a broadband acceleration, modelled as a white noise Gaussian stochastic process. Differently from [16], the mechanical system response statistics (namely the stationary joint state space probability density function) was derived from the Fokker-Planck-Kolmogorov (FPK) equation, as done in many references. It is stressed that the nonlinearity level cannot affect the electric power output, but it can reduce the amplitude of the maximum expected displacement. The maximum displacement is quantified in terms of exceedance probability P_f during an excitation time T. The results of the analysis were used for a constrained optimisation criterion where the mean value of the electric power is maximised under the constraint that the maximum displacement will not reach a given threshold during a time $t \in [0, T]$.

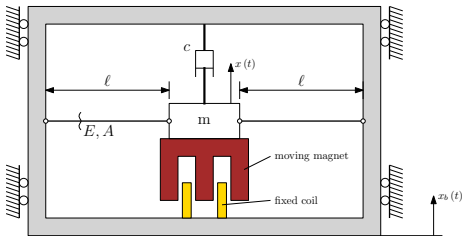

Figure 1: Sketch of the energy harvesting device. The mass, in white, is connected to the main case with two rods of length ℓ and can move vertically, only.

2. Problem formulation

A schematic of the mechanical component of a SDOF energy harvesting device with a cubic stiffness nonlinearity is shown in Figure 1. The mass, m, is connected to the main case (box) of the energy harvester with two linear elastic rods of length ℓ. The rods have cross-section area equal to A and are made of a material with Young's modulus E. The mass is connected to the main case also with a viscous damper. As the main case is excited, the suspended mass starts vibrating. The position of the main case is expressed through the coordinate $x_b\,(t)$, while the coordinate of the mass is $x\,(t)$. A moving coil connected to the mass and a magnet realise an electromagnetic coupling to transfer kinetic energy into the electrical domain (through Faraday's law). The device is connected to an electrical load resistance and to the circuit diagram shown in Figure 2. The coil can be modelled as an inductance L_i and an electric resistance R_i. The external load is sketched with resistance R_e, which accounts for the circuits to rectify the current and store it.

2.1. Nonlinear Duffing-type electromechanical equations of motion

The energy harvester can be modelled as system made of a mass connected to a moving base through a viscous damper and a nonlinear spring, as proved in the following. The mass connected with the two rods to the case can move laterally (up and down in the sketch of Fig. 1), only, and the coordinate x identifies its position. The null position corresponds to $x = 0$. As soon as

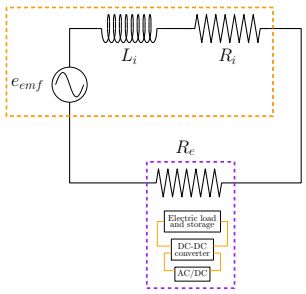

Figure 2: Sketch of the electric circuit of the energy harvesting device.

the mass moves, the length of the two rods varies. Considering that the mass position is x, the strain in the rods can be computed as

$$\varepsilon_{zz} = \frac{\ell(x) - \ell_0}{\ell_0} = \frac{\sqrt{\ell_0^2 + x^2} - \ell_0}{\ell_0}, \tag{1}$$

where $\ell(x)$ is the actual length of the rod. The square root at the numerator can be approximated with a McLaurin series expansion as

$$\sqrt{\ell_0^2 + x^2} = \ell_0 + \frac{x^2}{2\ell_0} - \frac{x^4}{8\ell_0^3} + \circ[x^6], \tag{2}$$

which simplifies into

$$\sqrt{\ell_0^2 + x^2} \equiv \ell_0 + \frac{x^2}{2\ell_0} \tag{3}$$

under small-displacements hypothesis. Substituting Eqn. (3) into Eqn. (1), the strain turns into

$$\varepsilon_{zz} \equiv \frac{x^2}{2\ell_0^2}. \tag{4}$$

The force in the prestressed rod, which is equal to N_0 in the null position, varies with the position of the mass as

$$N(x) = N_0 + EA\frac{x^2}{2\ell_0^2}. \tag{5}$$

The resultant force in the rods, which have an angle α with respect to the null position, is a restoring force that points towards the rest position and has magnitude

$$F = 2N\cos\alpha = 2\left[N_0 + EA\frac{x^2}{2\ell_0^2}\right]\frac{x}{\sqrt{\ell_0^2 + x^2}}. \tag{6}$$

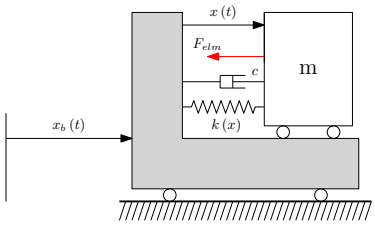

Figure 3: Sketch of the equivalent sigle degree-of-freedom system (SDOF).

The right-hand side fraction can be rewritten in terms of a McLaurin expansion as

$$\frac{x}{\sqrt{\ell_0^2 + x^2}} = \frac{x}{\ell_0} + \frac{x^3}{2\ell_0^3} + \frac{3x^5}{8\ell_0^5} + \circ[x^6]. \tag{7}$$

Under the hypothesis of small-displacements, the first term of Eqn. (7) can be considered, only. Hence, the restoring force F is equivalent to

$$F(x) = \frac{2N_0}{\ell_0} x + EA\frac{x^3}{\ell_0^3}. \tag{8}$$

The mass connected with the rods can be idealised as a single degree-of-freedom system (Figure 3) with a nonlinear mechanical stiffness $k(x)$ equal to

$$k(x) = k_0\left(x + \varepsilon x^3\right), \tag{9}$$

where

$$k_0 = \frac{2N_0}{\ell_0} \tag{10}$$

and

$$\varepsilon = \frac{EA}{2N_0\ell_0^2}. \tag{11}$$

Assuming that the inertial displacement is the sum of the relative displacement x plus the base displacement x_b, the inertial acceleration is $\ddot{x} + \ddot{x_b}$. Considering the contribution of the viscous damping $c\ddot{x}$ and the electromagnetic coupling force F_{elm}, the dynamic equilibrium equation of the vibrating mass is

$$m(\ddot{x} + \ddot{x_b}) + c\dot{x} + k_0(x + \epsilon x^3) + F_{elm} = 0. \tag{12}$$

Considering the inertial force due to the base displacement as forcing term, Eqn. (12) turns into

$$m\ddot{x} + c\dot{x} + k_0(x + \epsilon x^3) + F_{elm} = -m\ddot{x}_b. \tag{13}$$

2.2. Electromagnetic coupling force, F_{elm}

Adopting an electromagnetic coupling to transfer the kinetic energy to an electrical circuit by the Faraday's law and connecting the device to a load resistance, the simplest model we can use is sketched in Figure 2, where R_e is the load resistance, R_i is the coil resistance and L_i is the inductance. The electromechanical force F_{elm} acting on the mass m is the force on the centre magnet due to the electromagnetic coupling. From Faraday's law, one can write

$$E_{ind} = -\frac{d\Psi}{dt} = -\frac{d\Psi}{dx}\dot{x}, \tag{14}$$

where E_{ind} is the induced electromotive force and Ψ is the magnetic flux. Equating the instantaneous power between the mechanical and electrical domains, the following equality results

$$F_{elm}\dot{x} = iE_{ind}, \tag{15}$$

where i is the electric current flowing within the coil. Combining Eqns. (14) and (15), it results that that the electromagnetic force is

$$F_{elm} = -i\frac{d\Psi}{dx}. \tag{16}$$

Applying the Kirchoff's law to the electric circuit, the induced electromotive force is

$$E_{ind} = i\left(R_e + R_i\right) + L_i\frac{di}{dt}. \tag{17}$$

For low-frequency applications (such as the ones herein proposed for the energy harvesting device), the effect of the inductance L_i is negligible and Eqn. (17) simplifies in

$$E_{ind} = iR_{eq}, \tag{18}$$

where $R_{eq} = R_e + R_i$ is the equivalent electrical resistance of the system. Substituting Eqns. (18) and (14) into Eqn. (16), the electromagnetic force F_{elm} turns into

$$F_{elm} = \frac{d\Psi}{dx}\frac{\dot{x}}{R_{eq}}. \tag{19}$$

Finally, assuming that the rate of change of the flux is constant over the region of interest, Eqn. (19) can be further simplified in

$$F_{elm} = \alpha\frac{\dot{x}}{R_{eq}}, \tag{20}$$

where $\alpha = d\Psi/dx$.

Inserting the electromagnetic force of Eqn. (20) into Eqn. (13) and dividing by the mass m, the equation of motion turns into

$$\ddot{x} + 2\xi_{elm}\omega_0\dot{x} + \omega_0^2 x\left(1 + \epsilon x^2\right) = -\ddot{x}_b, \tag{21}$$

where

$$\xi_{elm} = \xi_0 + \frac{\alpha^2}{2\omega_0 m R_{eq}} \tag{22}$$

is the electromechanical damping ratio due to mechanical and magnetic phenomena. In detail, ξ_0 is the mechanical damping ratio, i.e, $\xi_0 = c/\left(2m\omega_0\right)$, while $\omega_0 = \sqrt{k/m}$ is the mechanical angular frequency. The second addend of Eqn. (22) represents the effect of the electromagnetic coupling and it is nonlinear with respect to R_{eq}. The mechanical damping ratio ξ_0 depends only on the mechanical configuration and it is constant.

3. Random vibration response to a broadband white noise excitation

The probabilistic response of a vibrational systems under Gaussian white noise random excitations, in general, can be considered to be governed by the following set of first-order stochastic differential equations (SDEs):

$$d\mathbf{Y}(t) = \mathbf{M}(\mathbf{Y})dt + \mathbf{G}(\mathbf{Y})d\mathbf{W}(t), \tag{23}$$

where $\mathbf{Y}(t)$ is a R^n valued stochastic process, while $\mathbf{M}(\mathbf{Y})$ and $\mathbf{G}(\mathbf{Y})$ are the drift vector and the diffusion matrix, respectively. The term $d\mathbf{W}(t)$ is the differential form of a n-dimensional vector of uncorrelated white noise, fully defined

by the first and second moments of its components given by,

$$E[W_i(t)] = E[W_j(t)] = 0, \tag{24}$$

$$E[W_i(t_1)W_j(t_2)] = 2\mathbf{D}_i\delta(\tau), \tag{25}$$

$$E[W_i(t)W_j(t)] = 0, \tag{26}$$

where $\tau = t_2 - t_1$, $\mathbf{D}_i$ is the spectral density of the excitation and $\delta(\tau)$ is the Dirac delta function, while $E[\cdot]$ denotes the expectation operator. The aforementioned system forms a Markov vector process in R^n, the behaviour of which is completely determined by the transition probability density function $p(\mathbf{Y}, t, |\mathbf{Y}_0)$. The transition probability density function is proportional to the probability of being in a differential element $(\mathbf{Y}, \mathbf{Y} + d\mathbf{Y})$ of the phase plane at time t, having started at $\mathbf{Y}_0$ at time zero, t_0, and satisfies both forward and backward Kolmogorov equations. The Fokker-Plank equation associated with Eqn. (23) can be derived from the Itô form. In more details, assuming that the base acceleration $\ddot{x_b}$ is a white noise Gaussian process, we can rearrange Eqn. (21) as

$$\dot{\mathbf{Y}} = \mathbf{f}\big(\mathbf{Y}, t\big) + \mathbf{G}\big(\mathbf{Y}, t\big)\mathbf{W}(t), \tag{27}$$

where the state vector $\mathbf{Y}(t)$ is

$$\mathbf{Y}(t) = \Big[\mathbf{X}(t), \dot{\mathbf{X}}(t)\Big]^T. \tag{28}$$

The vector $\mathbf{f}\big(\mathbf{X}, t\big)$ has components

$$\mathbf{f}_1 = Y_2 \tag{29}$$

and

$$\mathbf{f}_2 = -2\xi_{elm}\omega_0 Y_2 - \omega_0\left(Y_1 + \varepsilon Y_1^3\right), \tag{30}$$

and the vector $\mathbf{G}$ is

$$\mathbf{G} = \big[0, -1\big]^T, \tag{31}$$

assuming that

$$\mathbf{Y}(t_o) = \mathbf{Y}_o \qquad t \in [t_0, t]. \tag{32}$$

3.1. Stationary response

The electro-mechanical system described with Eqn. (21) is subjected to a stationary Gaussian white noise excitation $\mathbf{W}(t)$ with one-sided spectral density of intensity S_0. The probability density function associated to a given state $\left[\mathbf{X}(t), \dot{\mathbf{X}}(t)\right]^T$, namely $p_{X\dot{X}}(x, \dot{x})$, is obtained from by the Fokker-Plank equation [26] as

$$p_{X\dot{X}}(x, \dot{x}) = A \exp\Big[- \frac{1}{2\sigma_0}\Big(x_1^2 + \frac{\varepsilon}{2}x_1^4\Big) - \frac{x_2^2}{2\dot{\sigma}_0}\Big], \tag{33}$$

where σ_0 and $\dot{\sigma}_0$ are the standard deviations of $\mathbf{X}$ and $\dot{\mathbf{X}}$ for the associated linear system (i.e., the system with $\varepsilon = 0$), as

$$\sigma_0^2 = \frac{\pi S_0}{4\xi_{elm}\omega_0^3}, \tag{34}$$

$$\dot{\sigma}_0^2 = \frac{\pi S_0}{4\xi_{elm}\omega_0}, \tag{35}$$

while A is the normalisation constant that is computed as

$$A = \left[\pi\sqrt{\frac{S_0}{4\varepsilon\xi_{elm}\omega_0}} \exp\left(\frac{1}{8\varepsilon\sigma_0}\right) K_{1/4}\left(\frac{1}{8\varepsilon\sigma_0}\right)\right]^{-1} \tag{36}$$

where $K_{1/4}(\cdot)$ is the modified Bessel function of order $1/4$. Hence it results that

$$\int_{-\infty}^{+\infty}\int_{-\infty}^{+\infty} p_{X\dot{X}}(x, \dot{x}) dx d\dot{x} = 1. \tag{37}$$

3.2. Threshold crossing probability

Differently to other works, in this paper the target problem is the maximisation of the electric power generation under the constraint that the maximum displacement will not exceed a given threshold level, as for larger displacements damages to the system can be expected. This request holds if a nonlinear Duffing mechanical system is assumed, as this kind of nonlinearity only affects the displacement response without effects on velocity, as proven in this section.

The problem of identifying the exceedance of a given level can somehow traced back to the case of structural systems subjected to random loads which failure is associated to the process of crossing a given threshold β (e.g., in terms

of strength or displacement) during a predefined temporal interval T. In other words, the probability $P_f(T)$ of the first time crossing of a structural response $\mathbf{X}$ through a given threshold value β can be computed. For a generic single degree-of-freedom system subjected to a stationary stochastic process, $P_f(T)$ is equal to

$$P_f(T) = 1 - e^{-h(\beta)T}, \tag{38}$$

where $h(\beta)$ is the hazard function, or conditioned threshold crossing rate. In Rice's original formulation [27], the hazard function is expressed by

$$h(\beta) = \int_0^{+\infty} \dot{x} p_{X\dot{X}}(\beta, \dot{x}|Q) d\dot{x}, \tag{39}$$

being $p_{X\dot{X}}(\beta, \dot{x}|Q)$ the conditional joint probability density function of processes $X(t)$ and $\dot{X}(t)$, and Q the condition of absence of excursions beyond β before t.

By means of the Poisson assumption, the hazard function $h(\beta)$ can be replaced by the threshold crossing rate $\nu_{|X|}(\beta)$. In the following, since the involved process is the displacement $\mathbf{X}$ of the vibrating mass, the symbol related to the threshold crossing rate $\nu_{|X|}(\beta)$ is simplified into $\nu_{|\beta|}$, which is equal to

$$\nu_{|\beta|} = \nu_{\beta}^{+} + \nu_{-\beta}^{-} = 2\nu_{\beta}^{+}, \tag{40}$$

as the failure is due to a double symmetric threshold crossing, where β-upcrossing rate, ν_{β}^{+}, is equal to

$$\nu_{\beta}^{+} = \int_0^{+\infty} \dot{x} p_{X\dot{X}}(\beta, \dot{x}) d\dot{x}. \tag{41}$$

Considering the associated linear mechanical system ($\varepsilon = 0$) subjected to stationary Gaussian white noise processes, thanks to Eqn. (34), a dimensionless threshold η equal to

$$\eta = \frac{\beta}{\sigma_0} \tag{42}$$

can be defined. The mean η-upcrossing rate in the associated linear SDOF is

$$\hat{\nu}_{\eta,lin}^{+} = \frac{\omega_0}{2\pi} \exp\left(-\frac{1}{2}\eta^2\right). \tag{43}$$

The reliability evaluation through Eqn. (38) has some restrictions. It holds under the assumption of Poisson hypothesis for independent threshold crossings.

Actually, it is well known that this hypothesis can be quite poor and excessively conservative when clumping effects occur in barrier (threshold) crossings (more accurate approaches are for example those based on the knowledge of envelope processes statistics [28]). Moreover, it has been verified that Poisson hypothesis holds for high threshold levels [29]. Following that, the hypothesis could be herein used since high reliability levels are considered and, by consequence, the threshold upcrossing events could be effectively assumed as independent. Substituting the Duffing system probability density function of Eqns. (33) and (36) into Eqn. (41), the crossing rate related to the threshold η turns into

$$\nu_{\eta}^{+} = \sqrt{\frac{\psi}{\pi}} \frac{\omega_0}{\phi(\psi)} \exp\left[-\frac{1}{2}\left(\eta^2 + \frac{\psi}{2}\eta^4\right)\right], \tag{44}$$

where the nonlinearity is expressed in a more effective way by using the parameter $\psi = \varepsilon\sigma_0^2$. The term $\phi(\psi)$ is

$$\phi(\psi) = \frac{K_{1/4}\left(\frac{1}{8\psi}\right)}{\exp\left(-\frac{1}{8\psi}\right)}. \tag{45}$$

It emerges that the nonlinearity plays a central role in reducing the values of η, as illustrated in Figure 4, where the ratio between the crossing rate related to the Duffing system, Eqn. (44), over the crossing rate in the associated linear system, Eqn. (43), is plot versus η, showing clearly how the Duffing system threshold crossing rate decays for η greater than 1, compared with the corresponding linear one.

The probability that the maximum system displacement will exceed the bilateral displacement threshold $|\eta|$ is thus

$$P\left(\frac{|X|}{\sigma_0} < \eta, t \in [0,T]\right) = 1 - P_f = \exp\left(-T\nu_{|\eta|}\right), \tag{46}$$

where T is the duration of the excitation or, alternatively, the time interval we consider to verify the threshold crossing. The argument of the exponential function in Eqn. (46) depends on ε, which controls the decay rate of the probability of failure P_f, namely the probability that in the interval $[0,T]$ the maximum displacement exceeds the bilateral double threshold $|\eta|$, as shown in Figure 5

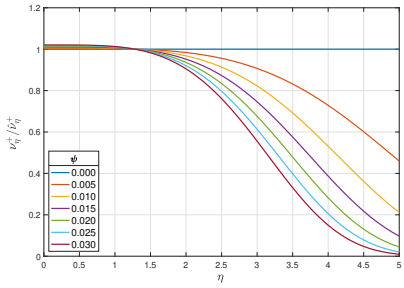

Figure 4: Ratio between η-upcrossing rate in Duffing system and η-upcrossing rate in the associated linear system versus the value of the dimensionless threshold η.

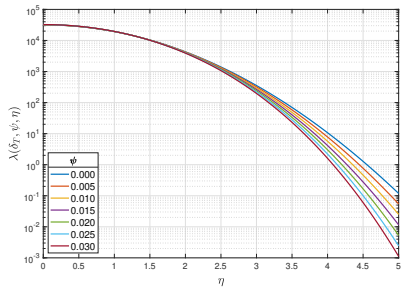

Figure 5: Influence of the nonlinearity for the parameter λ versus the dimensionless threshold η, for $2\pi\delta_T = 10^5$.

where the parameter $\lambda = T\nu_{|\eta|} = 2T\nu_\eta^+$ is plotted versus η. In detail, λ is expressed as

$$\lambda(\delta_T, \psi, \eta) = 4\delta_T \frac{\sqrt{\psi\pi}}{\phi(\psi)} \exp\left[-\frac{1}{2}\left(\eta^2 + \frac{\psi}{2}\eta^4\right)\right], \tag{47}$$

where the parameter $\delta_T = T\omega_0/2\pi$ is the number of vibration cycles of the associated linear system over the duration T. Substituting Eqn. (47) in Eqn. (46), the failure probability is obtained as

$$P_f = 1 - \exp\big[-\lambda(\delta_T, \psi, \eta)\big]. \tag{48}$$

Figure 6 shows the influence of ψ on the value of the failure probability P_f versus the dimensionless threshold η, for $2\pi\delta_T = 10^5$. Eqn. (48) can be inverted to obtain the dimensionless threshold value η with respect to the failure

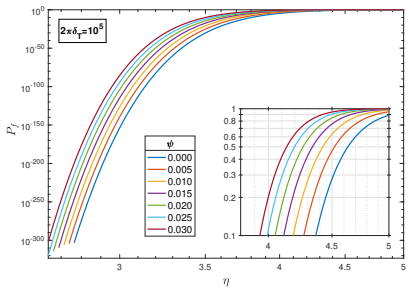

Figure 6: influence of nonlinearity for the probability of failure P_f versus the dimensionless threshold η, for $2\pi\delta_T = 10^5$.

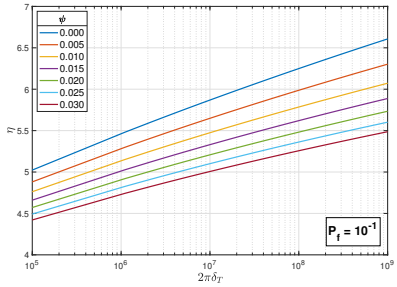

Figure 7: Maximum dimensionless threshold sensitivity for different values of parameter ψ versus $2\pi\delta_T$ assuming $P_f = 0.1$. The curve $\psi = 0$ corresponds to the associated linear SDOF system.

probability P_f, as

$$\eta(\delta_T, \psi, P_f) = \sqrt{\frac{1}{\psi}\sqrt{1 - 4\psi \ln\left(-\frac{\phi(\psi)\ln(1-P_f)}{4\delta_T\sqrt{\psi\pi}}\right)} - 1}. \tag{49}$$

In Figures 7, 8 and 9 the sensitivity of the dimensionless threshold level η for different number of cycles δ_T is illustrated for different values of P_f.

3.3. Mean value of the generated electric power

The deterministic value of the electrical power is calculated from the instantaneous power given in Eqn. (15) as

$$iE_{ind} = F_{elm}\dot{x} = \frac{\alpha^2\dot{x}^2}{R_{eq}}. \tag{50}$$

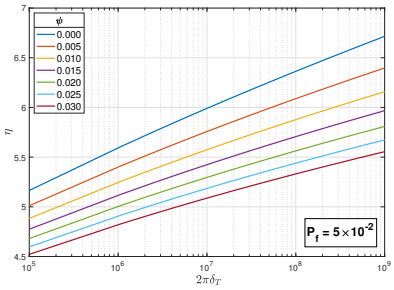

Figure 8: Maximum dimensionless threshold sensitivity for different values of parameter ψ versus $2\pi\delta_T$ assuming $P_f = 0.05$. The curve $\psi = 0$ corresponds to the associated linear SDOF system.

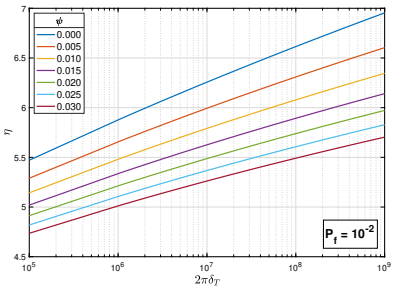

Figure 9: Maximum dimensionless threshold sensitivity for different values of parameter ψ versus $2\pi\delta_T$ assuming $P_f = 0.01$. The curve $\psi = 0$ corresponds to the associated linear SDOF system.

The square of the current in the circuit, considering the hypothesis of negligible inductance of Eqn. (18), is

$$i^2 = \frac{\alpha^2 \dot{x}^2}{R_{eq}^2}, \tag{51}$$

and, finally, the deterministic value of the electric power over the external resistance is

$$P_{load} = \frac{R_e \alpha^2 \dot{x}^2}{R_{eq}^2}. \tag{52}$$

As shown in Eqn. (52), the power through the load resistor R_e is proportional to the square of the relative velocity of the moving magnet. The expected value of the relative velocity squared is insensitive to the Duffing type nonlinearities, as ξ_{elm} in Eqn. (35) does not depend on ε. We found that the mean value of the electric power of Eqn. (52) is

$$\langle P_{load} \rangle = \dot{\sigma}_0^2 \frac{R_e \alpha^2}{R_{eq}^2}. \tag{53}$$

Considering Eqns. (35) and (22), we have finally that

$$\langle P_{load} \rangle = S_0 \frac{\pi \alpha^2 R_e}{4\omega_0 \xi_0 R_{eq}^2 + 2\frac{\alpha^2}{m} R_{eq}}. \tag{54}$$

4. Optimal design

As a results of the calculations reported in Sec. 3, although the term ε implicitly controls the probability of exceeding a given displacement (threshold), the performance of the energy harvester is not affected by the nonlinearity of the mechanical system. Following this result, the present section proposes an optimisation strategy with the aim to maximise the energy performance of the energy harvester, but imposing a limitation to the maximum displacement of the vibrating mass (i.e. the moving magnet).

The optimisation problem is stated assuming a design vector $\mathbf{b}$ (listing the parameters to be optimised)

$$\mathbf{b} = \begin{pmatrix} R_e \\ \omega_0 \end{pmatrix} \tag{55}$$

as representative of the electric and mechanical design of device. The Objective Function (OF) is the mean value of the electric power, represented by Eqn. (54).

To solve the optimisation problem, a partial derivative of the OF with respect to the external resistance R_e, which is an element of the design vector, is performed to check if stationary points are present. It results that

$$\frac{\partial \mathrm{OF}(\mathbf{b})}{\partial R_e} = S_0 \frac{\pi \alpha^2 m \left[2m\xi_0\omega_0(R_i^2 - R_e^2) + \alpha^2 R_i\right]}{2(R_i + R_e)^2 \left[\alpha^2 + 2m\xi_0\omega_0(R_i + R_e)\right]^2}, \tag{56}$$

which is a monotonically increasing function for decreasing values of ω_0, becoming asymptotically $+\infty$ for $\omega_0 \longrightarrow 0$. Zeroing the derivative of the OF, Eqn. (56), with respect of R_e, the optimal external resistance R_e^{opt} is found

$$R_e^{opt} = \sqrt{R_i \left(R_i + \frac{\alpha^2}{2m\omega_0\xi_0}\right)}. \tag{57}$$

The resistance R_e^{opt} is dependent on ω_0. As a result, a reduction of ω_0 (i.e., a reduction of the mechanical stiffness k of the system) would increase the energy efficiency, with the undesirable effect of increasing displacements. The mean electric power obtained with the optimal external resistance is obtained by substituting Eqn. (57) into Eqn. (54), resulting in

$$\langle P_{load} \rangle = S_0 \frac{\pi m}{2} \left(1 - \frac{\sqrt{\gamma\left(\alpha^2 + \gamma\right)} - \gamma}{\alpha^2}\right), \tag{58}$$

where $\gamma = 2R_i m\omega_0\xi_0$. As an example, Figure 10 plots Eqns. (58) and (57) for different values of the angular frequencies ω_0 on a given set of variables $(\xi_0, S_0, m, \alpha, R_i)$, as reported in the caption of the figure. It is observed that the mean electric power is monotonically decreasing with the increase of ω, confirming that high powers are obtained with systems that have low mechanical stiffness. Eqn. (58) represents the best mean electric power that can be produced if the mechanical system has a given angular frequency ω_0. To achieve such power, an external load of resistance computed with Eqn. (57) must be adopted.

For a given set of parameters $(\xi_0, S_0, m, \alpha, R_i)$, if the external resistance R_e is provided the optimal angular frequency ω_0^{opt} for which the mean electric power is maximised is

$$\omega_0^{opt} = \frac{R_i \alpha^2}{2m\xi_0 \left(R_e^2 - R_i^2\right)}, \tag{59}$$

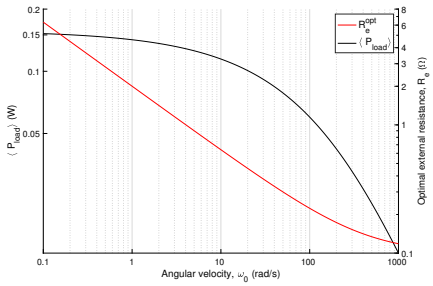

Figure 10: Mean electric power $\langle P_{load} \rangle$ and optimal external resistance R_e^{opt} for different values of ω_0. Parameters are $\xi_0 = 0.05$, $S_0 = 10$ $(\mathrm{m/s^2})^2/\mathrm{Hz}$, mass $m = 0.01$ kg, $\alpha = 0.2$ Wb/m and coil resistance $R_i = 0.1$ Ω.

provided that $R_i^2 \leq R_e^2$ and the resulting $\langle P_{load} \rangle$ is

$$\langle P_{load} \rangle = S_0 \frac{m\pi \left(R_e - R_i\right)}{2R_{eq}}. \tag{60}$$

Eqn. (60) represents the best mean electric power that can be produced if the electrical system has an electric load of resistance R_e. To achieve such power, the angular frequency of the mechanical system must satisfy Eqn. (59).

Knowing the duration of the process, T, once the required reliability level is fixed (probability of failure P_f and maximum acceptable displacement, i.e. the target displacement threshold $\tilde{\beta}$), by iteration, the correct value of the nonlinear term ε can be determined. In detail, the dimensionless target displacement threshold is $\tilde{\eta} = \tilde{\beta}/\sigma_0$. Adopting a trial value of ε, the tentative η is computed with Eqn. (49), until convergence (the larger the ε, the smaller the η, as plotted in Figures 7, 8 and 9).

The main steps of the procedure are here summarised:

1. define $\xi_0, S_0, m, \alpha, R_i$ based on technical constraints (vibration source, available mass, coil type and characteristics). Define the target displacement threshold $\tilde{\beta}$ and the failure probability P_f;

2a. if R_e is known, use Eqns. (59) and (60) to define the angular frequency ω and mean electric power $\langle P_{load} \rangle$, respectively; or,

2b. if ω_0 is known, use Eqns. (57) and (58) to define the external load resistance R_e and mean electric power $\langle P_{load} \rangle$, respectively;

Table 1: SDOF system properties.

Parameter	Value
m	0.01 kg
ω_0	10 rad/s
ξ_0	0.05
ε	0.5
α	0.2 Wb/m
R_i	0.5 Ω
R_e	1.5 Ω
S_0	2.4 $(\mathrm{m/s^2})^2/\mathrm{Hz}$
T	10 s

3. compute σ_0 with Eqn. (34) and the target $\tilde{\eta} = \tilde{\beta}/\sigma_0$;
4. define nonlinear term ε iteratively, until the term η computed with Eqn. (49) equals the target $\tilde{\eta}$.

4.1. An example of application

To check the validity of the previous formulae, an example of application is proposed. A single degree-of-freedom electro-mechanical system with Duffing-type nonlinearity subjected to a Gaussian white noise random excitation having the properties reported in Table 1 is considered. The duration of the excitation is 10 s. The values of ω and R_e are the ones that satisfy Eqns. (59) and (57) to maximise the mean electric power. A threshold displacement equal to $\tilde{\beta} = 0.35$ m is fixed. It is required to compute threshold exceeding probability.

First, the electromechanical damping ratio is computed through Eqn (22), resulting in $\xi_{elm} = 0.15$. The variance of mass displacement and mass velocity are computed with Eqns. (34) and (35), respectively, as $\sigma = 0.11$ m and $\dot{\sigma} = 1.12$ m/s. The normalized threshold displacement is $\eta = 3.12$ and the total number of cycles in the equivalent elastic system is $\delta_T = 15.19$. Adopting Eqns. (47) it results $\lambda = 0.21$, from which the threshold exceedance probability P_f is determined. Thanks to Eqn. (48), it results $P_f = 0.18$.

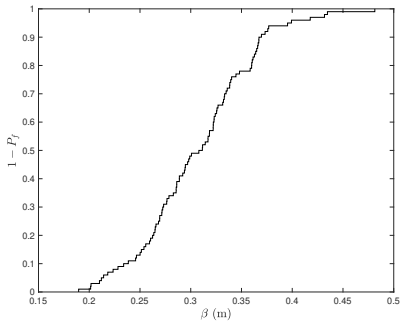

Figure 11: Empirical cumulative density function .

To check the validity of the analytical solution, a set of 100 different simulations of the system subjected to 10 s-long Gaussian white noise with a frequency sampling of 50 Hz were performed. The response of the system was evaluated by integrating the second order differential equation, Eqn. (21). The maximum absolute displacement in each simulation was recorded. Figure 11 plots the empirical cumulative probability distribution of the maxima: the survival probability corresponding to $\tilde{\beta} = 0.35$ m is around 80%, from which it results that the exceeding threshold probability is 20%, confirming the result obtained through the analytical calculations.

5. Conclusions

The present papers deals with the solution of a nonlinear energy harvester with a Duffing-type nonlinearity subjected to a Gaussian white noise random excitation. A simple single degree-of-freedom electro-mechanical system is considered to develop all the calculations. The first-order stochastic differential equations are reported and solved to get the solution of the system. Attention towards the maximum displacement of the mechanical system is considered. To this aim, threshold crossing probability is considered and related to the failure probability of the system, which represents a design request. It is shown that mechanical nonlinearity does not affect the power production of the energy harvester, while it controls the probability of exceeding a given displacement.

To optimise the performance of the energy harvester subjected to a Gaussian white noise random excitation, the impedance matching principle, which serves for maximising power transfer and is commonly used in the design of the electrical circuit of energy harvesting devices [30], is here by-passed through an analytical optimisation model that accounts for the electromechanical coupling. The probability of exceeding a given threshold displacement is one of the constraints of the optimisation problem. It is shown that the optimisation procedure can be solved in two separate steps. First, the optimal load resistance is determined for a known undamped vibration frequency (of the associated linear oscillator), of the optimal undamped vibration frequency is determined for a known load resistance. Then, the value of the Duffing-type nonlinearity that satisfies the threshold displacement with the target failure probability is computed.

The proposed model and solutions allow to design an energy harvesting system tailored for a specific electrical device powered with ambient vibrations characterised by a broadband frequency bandwidth. The outputs of the research can be largely adopted for self-standing small structural health monitoring tools with MEMS technology.

References

[1] F. R. Fan, W. Tang, Z. L. Wang, Flexible nanogenerators for energy harvesting and self-powered electronics, Advanced Materials 28 (22) (2016) 4283–4305.

[2] H. Fu, X. Mei, D. Yurchenko, S. Zhou, S. Theodossiades, K. Nakano, E. M. Yeatman, Rotational energy harvesting for self-powered sensing, Joule 5 (5) (2021) 1074–1118.

[3] T. Nagayama, S.-H. Sim, Y. Miyamori, B. Spencer Jr, Issues in structural health monitoring employing smart sensors, Smart Structures and Systems 3 (3) (2007) 299–320.

[4] S. P. Beeby, M. J. Tudor, N. M. White, Energy harvesting vibration sources for microsystems applications, Measurement Science and Technology 17 (12) (2006) R175.

[5] A. Harb, Energy harvesting: State-of-the-art, Renewable Energy 36 (10) (2011) 2641–2654.

[6] S. Priya, D. J. Inman, Energy Harvesting Technologies, Vol. 21, Springer, 2009.

[7] S. P. Beeby, T. O'Donnell, Electromagnetic energy harvesting, Energy Harvesting Technologies (2009) 129–161.

[8] S. Roundy, P. K. Wright, J. Rabaey, A study of low level vibrations as a power source for wireless sensor nodes, Computer Communications 26 (11) (2003) 1131–1144.

[9] N. G. Stephen, On energy harvesting from ambient vibration, Journal of Sound and Vibration 293 (1-2) (2006) 409–425.

[10] S. Adhikari, M. Friswell, , D. Inman, Piezoelectric energy harvesting from broadband random vibrations, Smart Materials and Structures 18 (11) (2009) 115005.

[11] L. Gammaitoni, I. Neri, H. Vocca, Nonlinear oscillators for vibration energy harvesting, Applied Physics Letters 94 (16) (2009) 164102.

[12] N. Tran, M. H. Ghayesh, M. Arjomandi, Ambient vibration energy harvesters: A review on nonlinear techniques for performance enhancement, International Journal of Engineering Science 127 (2018) 162–185.

[13] R. Ahmed, F. Mir, S. Banerjee, A review on energy harvesting approaches for renewable energies from ambient vibrations and acoustic waves using piezoelectricity, Smart Materials and Structures 26 (8) (2017) 085031.

[14] E. K. Reilly, L. M. Miller, R. Fain, P. Wright, A study of ambient vibrations for piezoelectric energy conversion, Proc. PowerMEMS 2009 (2009) 312–315.

[15] R. Bobryk, D. Yurchenko, Enhancing energy harvesting by a linear stochastic oscillator, Probabilistic Engineering Mechanics 43 (2016) 1–4.

[16] I. Petromichelakis, A. F. Psaros, I. A. Kougioumtzoglou, Stochastic response determination and optimization of a class of nonlinear electromechanical energy harvesters: A wiener path integral approach, Probabilistic Engineering Mechanics 53 (2018) 116–125.

[17] H. Wenzel, D. Pichler, Ambient Vibration Monitoring, John Wiley & Sons, 2005.

[18] L. Tang, Y. Yang, C. K. Soh, Toward broadband vibration-based energy harvesting, Journal of Intelligent Material Systems and Structures 21 (18) (2010) 1867–1897.

[19] J. Twiefel, H. Westermann, Survey on broadband techniques for vibration energy harvesting, Journal of Intelligent Material Systems and Structures 24 (11) (2013) 1291–1302.

[20] M. F. Daqaq, Response of uni-modal duffing-type harvesters to random forced excitations, Journal of Sound and Vibration 329 (18) (2010) 3621–3631.

[21] P. Kumar, S. Narayanan, S. Adhikari, M. Friswell, Fokker–planck equation analysis of randomly excited nonlinear energy harvester, Journal of Sound and Vibration 333 (7) (2014) 2040–2053.

[22] P. Green, K. Worden, K. Atallah, N. Sims, The benefits of Duffing-type nonlinearities and electrical optimisation of a mono-stable energy harvester under white gaussian excitations, Journal of Sound and Vibration 331 (20) (2012) 4504–4517.

[23] Y. Jin, Y. Zhang, Dynamics of a delayed Duffing-type energy harvester under narrow-band random excitation, Acta Mechanica 232 (3) (2021) 1045–1060.

[24] Q. He, M. F. Daqaq, Electric load optimization of a nonlinear mono-stable duffing harvester excited by white noise, Meccanica 51 (5) (2016) 1027–1039.

[25] B. D. Truong, C. P. Le, E. Halvorsen, Power optimization and effective stiffness for a vibration energy harvester with displacement constraints, Journal of Micromechanics and Microengineering 26 (12) (2016) 124006.

[26] T. T. Soong, M. Grigoriu, Random vibration of mechanical and structural systems, Prentice Hall, 1993.

[27] S. O. Rice, Mathematical analysis of random noise, The Bell System Technical Journal 23 (3) (1944) 282–332.

[28] W. D. Iwan, P.-T. Spanos, Response envelope statistics for nonlinear oscillators with random excitation, Journal of Applied Mechanics 45 (1978) 170–174.

[29] S.-r. Yi, J. Song, First-passage probability estimation by Poisson branching process model, Structural Safety 90 (2021) 102027.

[30] H. Jabbar, H. J. Jung, N. Chen, D. H. Cho, T. H. Sung, Piezoelectric energy harvester impedance matching using a piezoelectric transformer, Sensors and Actuators A: Physical 264 (2017) 141–150.